Structure of the liquid and the crystal of the phase-change material SnSe₂:
First-principles molecular dynamics

M. Micoulaut,[1] W. Wełnic,[2,3] and M. Wuttig[4,5]

[1]*Laboratoire de Physique Théorique de la Matière Condensée, UPMC, Paris 6, Boîte 1214,*
Place Jussieu, 75252 Paris Cedex 05, France
[2]*Laboratoire des Solides Irradiés, CNRS-CEA, École Polytechnique, 91128 Palaiseau, France*
[3]*European Theoretical Spectroscopy Facility (ETSF)*
[4]*Physikalisches Institut (IA), RWTH Aachen University of Technology, D52056 Aachen, Germany*
[5]*JARA—Fundamentals of Future Information Technology, RWTH, Aachen University, 52056 Aachen, Gernany*

First-principles molecular dynamics simulations are used to study the structural properties of liquid and crystalline SnSe₂. We reproduce the experimental structure factor with confidence and fully describe the pair-correlation functions and the local structure of the liquid. It is shown that, unlike other group IV chalcogenides such as GeSe₂, SnSe₂ does not display tetrahedral ordering in the liquid and contains a large amount of fivefold tin atoms with selenium atoms lying in an equatorial plane and at the edges of the polyhedra. A certain number of homopolar defects are found whose rate is substantially lower however than in GeSe₂. Compared to the crystalline system the density in the liquid decreases by 8.5%, which is accompanied by a decrease in the atomic coordination. Local distortions as found in typical phase-change materials are present in SnSe₂.

I. INTRODUCTION

Chalcogenide alloys have become an established class of materials in optical data storage during the last two decades.[1] They are used as so-called phase-change materials (PCMs) for applications requiring a reversible storage mechanism. Upon laser heating they switch rapidly and reversibly from the amorphous to the crystalline state.[2,3] This phase transition leads to significant changes in the optical reflectivity enabling data storage applications. Furthermore the resistivity changes by several orders of magnitude.[4] As the phase transition can also be accomplished by a current pulse instead of a laser pulse there is growing interest in employing PCMs for nonvolatile electronic data storage in phase-change random access memory (PCRAM) devices.[5–8]

So far mainly tellurides have been studied for their storage properties, in particular ternary compounds containing Ge and Sb as well as silver tellurides such as AgInSbTe. Recently new alloys such as GeSbSe (Ref. 9) and SnSe₂ (Ref. 10) have been shown to possess suitable properties for data storage based on the amorphous to crystalline phase transition. In order to optimize the search for suitable alloys it is desirable to identify compositional or stoichiometric trends for important properties. For the GeSbTe alloys this has been done, e.g., for the glass transition temperature T_g (Ref. 11) and for the optical properties.[12] However, in order to establish these trends detailed studies of the newly identified phase-change materials are required. Compared to GeSbTe alloys, the physical properties of SnSe₂, for example, are relatively unknown. Hence in the following we discuss the structural properties of this alloy and compare them to typical PCMs as well as to GeSe₂, which is chemically very similar but cannot be applied for data storage due to its glass-forming properties.[13]

SnSe₂ shows similar material characteristics than GeSbTe alloys. The resistivity contrast between the crystalline and the amorphous phase amounts to 5 orders of magnitude. The activation energy for crystallization is with 1.93 eV in the same range as for typical GeSbTe alloys. In addition, there is a pronounced density contrast between the crystalline and the amorphous phase,[10] which is larger than the density change typically observed for GeSbTe alloys.[14] On the other hand, the optical contrast is rather low and the recrystallization process is comparably slow. This might be due to the fact that the ratio of the glass transition and melting temperature T_g/T_M is slightly higher (0.55) than typical GeSbTe alloys ($T_g/T_M \simeq 0.5$).[15] In summary, SnSe₂ resembles but also deviates from generic phase-change material. It appears therefore as a very interesting system lying at the boundary of phase-change properties from which one can learn.

There are however several additional and more fundamental motivations for the present study. First, inspection of the Periodic Table shows that SnSe₂ is an isochemical compound of GeSe₂. One may therefore wonder if there are any differences in the liquid state, and if theoretical models of SnSe₂ will show the same kind of features as GeSe₂ which has been extensively studied both from classical[16,17] and first-principles molecular dynamics.[18–20] Since SnSe₂, unlike GeSe₂, shows some interesting properties concerning the phase-change behavior, it is certainly interesting to track the structural differences as a clue for the understanding of the phase-change properties. Second, little is known about the structure of the liquid and amorphous SnSe₂ among which the bond lengths and/or the bond angle distribution (see however Refs. 21 and 22). Is there any chemical or topological ordering of the liquid on different (short and intermediate) length scales? Are there any homopolar defects as in other chalcogenides? First-principles molecular dynamics can help us to provide insight on the basis of an electronic model.

This paper is organized as follows. In Sec. II, we detail the model employed to describe the structure of liquid and

crystalline $SnSe_2$. We then focus on the structure of the liquid by computing the structure factor and analyzing its features in detail, together with the local coordination numbers, bond angle distributions and pair-correlation functions that give access to the interatomic bond distances. We then turn to the analysis of the crystalline state and draw analogies between both phases. All along the paper, we compare the present system with the $GeSe_2$ benchmark and finally sketch some arguments about the observed volume contraction between the crystalline and the amorphous phase.

II. SIMULATION DETAILS

The investigation of the liquid and the crystalline states has been undertaken with different theoretical schemes, both based on the density-functional theory (DFT). The system used for the study of the liquid state consists of 120 atoms (40 Sn and 80 Se) in cubic cell with fixed length and periodic boundary conditions. The size of the cell has been taken as 15.34 Å in order to recover the experimental density of the liquid at 1173 K.[23] The electronic structure has been described within DFT which evolves self-consistently during the motion[24] using a generalized gradient approximation (GGA) for the exchange correlation.[25] Valence electrons have been treated explicitly using a Becke-Lee-Yang-Parr (BLYP) norm-conserving pseudopotential accounting for core-valence interactions.[26] The wave functions have been expanded at the Γ point of the supercell on a plane-wave basis set with energy cutoff of R_c=20 Ry. The size of the system appears to be rather well suited to address most issues related with short- and intermediate-range orders. In various liquid Ge-Se alloys, a 120 atom simulation could indeed reproduce[27,28] very accurately the scattering functions obtained from neutron diffraction. Recently, first-principles molecular dynamics has also been undertaken[29] on liquid B_2S_3 with system sizes of 80 and 320 atoms. The results of the pair distribution functions g_{B-B}, g_{B-S}, and g_{S-S} showed no differences between both system sizes. These few examples give us confidence in the reliability of the results obtained from a 120 atom liquid $SnSe_2$.

Structural analysis has been performed over a trajectory of 40 ps with a time step of 0.1 fs. A 10 ps simulation has been also undertaken with a larger cutoff for the plane-wave basis set (R_c=40 Ry) that showed no significant differences in both structure factors and pair-correlation functions. It parallels therefore similar obtained behavior for germanium chalcogenides for which the convergence of the structure factor is achieved within the same range[19] of R_c. Subsets of 10 ps each were taken to check for the consistency of the results. A typical snapshot of the liquid structure is given in Fig. 1.

The DFT calculations on the crystalline phase have been performed using the ABINIT code[30,31] based on plane waves and pseudopotentials. All calculations have been done in GGA for the exchange-correlation potential in the Perdew-Burke-Ernzerhof parametrization.[32] A $6\times6\times6$ Monkhorst-Pack grid has been employed for the summation over the Brillouin zone, and total-energy convergence has been achieved at an energy cutoff of 60 Ry.

FIG. 1. Snapshot of the 120 atom liquid $SnSe_2$ at 1173 K. Selenium atoms are in black. Note the presence of edge-sharing units (four rings) in the structure.

III. STRUCTURAL PROPERTIES

A. Structure factors

The total structure factor $S(q)$ of the liquid $SnSe_2$ system is displayed in Fig. 2 and does not differ significantly from the one calculated with R_c=40 Ry. It shows a relatively good agreement with the experimental data[21] in the low wave-vector region. One can however notice that in the higher wave-vector region, the peak appearing at q =5.5 Å^{-1} is slightly overestimated, and the small one observed at 7.2 Å^{-1} is shifted in the simulation to 8 Å^{-1}. Concerning the global shape of the structure factor, we should stress that it is not the one of a typical octahedral liquid as it contains two principal peaks of similar heights (here q=2.2 and 5.5 Å^{-1}) as for a tetrahedral system. This is not only true for the present experimental and theoretical structure factor $S(q)$ but also highlighted from various theoretical models. For instance, we have represented in Fig. 3 for comparison the present $S(q)$ of $SnSe_2$ together with the total structure factor of the simulated liquids $GeSe_2$ (Ref. 18) and $G_1Sb_2Te_4$.[33] The former is a typical tetrahedral liquid while the latter is known to be of octahedral type. Figure 3 shows that the $SnSe_2$ bears some similarities with the two systems.
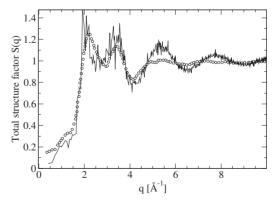

FIG. 2. Total neutron structure factor $S(q)$ for liquid $SnSe_2$ at 1173 K, compared to experiments (Ref. 21) (circles).
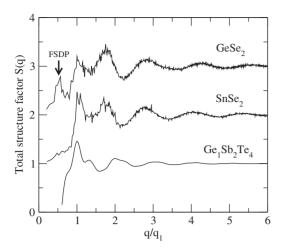
FIG. 3. Comparison of three simulated total structure factors: the present SnSe$_2$, tetrahedral GeSe$_2$ (Ref. [18]), and the octahedral Ge$_1$Sb$_2$Te$_4$ liquid (Ref. [33]). The first peak in the GeSe$_2$ curve is the first sharp diffraction peak.

Octahedral liquids usually display a prominent peak in the structure factor[34] whereas the $S(q)$ of tetrahedral liquids contains two main peaks, apart from the first sharp diffraction peak (FSDP), and the height of the peak lying at low wave vector is usually lower. Here, one can see that the structure factor of SnSe$_2$ has two peaks like in GeSe$_2$. However, the second peak (at $q = 1.6q_1$) is lower in intensity as for an octahedral liquid.

On the origin of the principal peak at 2.2 Å^{-1}, the conclusion of the experimental study[21] of the changes in $S(q)$ with tin composition was suggesting that it may mostly arise from Sn-Sn correlations as its position remains constant for all composition and its height increases with tin composition in the binary Sn$_x$Se$_{1-x}$. The detail of the calculated Faber-Ziman (FZ) partial structure factors (Fig. [4]) allows us to gain insight into the atomic dependent structural correlations. Here one sees that, in fact, the first peak clearly arises not only from the $S_{SnSn}(q)$ but also from $S_{SeSe}(q)$ partials because the latter displays also a first sharp peak at a wave vector somewhat higher than 2 Å^{-1}. The origin of the oscillations seen from the theoretical total structure factor $S(q)$ at higher wave vector (e.g., 5.5 and 8 Å^{-1}) clearly originates from the $S_{SnSe}(q)$ partial.
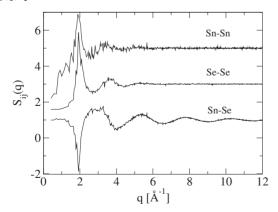

FIG. 4. Faber-Ziman partial structure factors of liquid SnSe$_2$ at 1173 K.
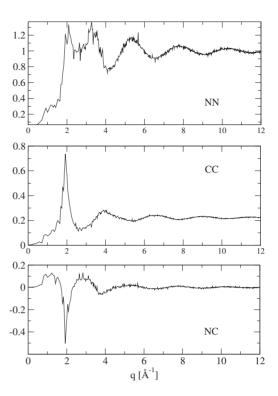

FIG. 5. Calculated Bhatia-Thornton partial structure factors of liquid SnSe$_2$ at 1173 K.

Additional analysis of the comparison between theoretical and experimental structure factors (Fig. [2]) is provided by an alternative means of representing $S(q)$. Bhatia-Thornton (BT) structure factors[35] emphasize either on topological or chemical ordering via a number-number $S_{NN}(q)$ and a charge-charge $S_{CC}(q)$ correlation. The total structure factor $S(q)$ then reads, depending on the representation (BT or FZ),

$$S(q) = S_{NN}(q) + A[S_{CC}(q)/c_{Sn}c_{Se} - 1] + BS_{NC}(q)$$
$$= c_{Sn}^2 b_{Sn}^2[S_{SnSn}(q) - 1] + 2c_{Sn}c_{Se}b_{Sn}b_{Se}[S_{SnSe}(q) - 1]$$
$$+ c_{Se}^2 b_{Se}^2[S_{SeSe}(q) - 1], \qquad (1)$$

where $A = c_{Sn}c_{Se}\Delta b^2/\langle b \rangle^2$, $B = 2\Delta b/\langle b \rangle$, $\Delta b = b_{Sn} - b_{Se}$, and $\langle b \rangle = c_{Sn}b_{Sn} + c_{Se}b_{Se}$. The last partial structure factor denoted $S_{NC}(q)$ focuses on correlations between number and concentration fluctuations.[36,37] Here, $b_{Sn} = 6.23$ fm and $b_{Se} = 7.97$ fm are the respective coherent scattering lengths of tin and selenium with concentration $c_{Sn} = 0.33$ and $c_{Se} = 0.67$. The BT structure factors can be determined by a linear combination of the FZ structure factors and details about the representation can be found in a review by Salmon.[38] For instance, $S_{NN}(q)$ is given by

$$S_{NN}(q) = c_{Sn}^2 S_{SnSn}(q) + c_{Se}^2 S_{SeSe}(q) + 2c_{Sn}c_{Se}S_{SeSe}(q). \quad (2)$$

The simulated BT structure factors are represented in Fig. [5]. They show that the main contribution to $S(q)$ arise from the number-number correlations, i.e., the global shape of the experimental and theoretical $S(q)$ is dominated by topology via the $S_{NN}(q)$ partial and depends rather weakly on the others [e.g., $S_{CC}(q)$ representative of chemical ordering]. This is not surprising. Indeed, from the definition of the quantities ap-
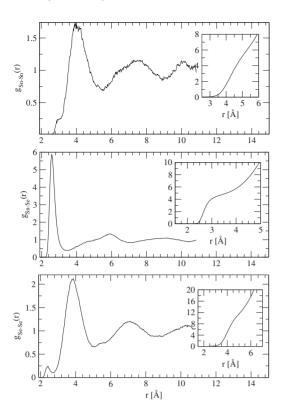
FIG. 6. Partial pair-correlation function for liquid SnSe$_2$ at 1173 K. The inset shows the corresponding running coordination numbers $n_{ij}(r)$.

pearing in Eq. (1), one has $A=0.0122$ and $B=0.4705$, i.e., $S_{NN}(q)$ appears to be a rather fair reproduction of the total structure factor. This arises not only from the close values of the scattering lengths of tin and selenium that lead to a low Δb but also from the fact that $S_{NC}(q)$ has a variation that is much smaller (Fig. 5) and a lower coefficient B when compared to $S_{NN}(q)$.

In this respect, it is tempting to conclude that liquid SnSe$_2$ seems rather similar to GeSe$_2$ because the latter displays also[18,39] the approximation $S(q) \simeq S_{NN}(q)$ with respective A and B values of 1.6×10^{-4} and 0.053. There are, however, more subtle differences with the germanium compound in q space. In fact, we note the quasiabsence of a FSDP in the experimental structure factor of SnSe$_2$, whereas it is obtained for GeSe$_2$ at similar temperatures of the liquid[40] (see also Fig. 3). In the present simulated system, we can only (but clearly) attribute a shoulder of the principal peak located at 1.2 Å^{-1} to an emerging FSDP, which is also seen in experiment (Fig. 2) and in amorphous thin films.[22] A temperature study of the experimental scattering function $S(q)$ shows that this shoulder grows to a well-separated peak[21] when the temperature is decreased, consistently with the usual temperature dependence of the FSDP in bulk glass-forming liquids.[41]

B. Pair-correlation functions

The different pair-correlation functions $g_{ij}(r)$ are displayed in Fig. 6. We also give in Table I the corresponding peak positions (i.e., bond distances) and coordination numbers n_{ij} computed at the first minimum of the pair distribu-

TABLE I. Interatomic distances (in Å) for liquid and crystalline SnSe$_2$, compared to experiment. Note that the Sn-Sn and Se-Se distances in the liquid could not be resolved from neutron diffraction (Ref. 21). In the crystalline phase two distinct positions can be found in the second-neighbor shell of Se.

	Sn-Sn(1)	Sn-Sn(2)	Sn-Se	Se-Se(1)	Se-Se(2)
			Liquid		
(Å)	3.00	3.92	2.57	2.42	3.87
Ref. 21 (Å)		3.88	2.68		3.88
n_{ij}	0.08	6.34	4.78	0.10	12.09
			Crystal		
(Å)		3.91	2.76		3.85/3.90
Ref. 42 (Å)		3.88	2.68		3.88

tion function. Neutron diffraction[21] is able to determine only an approximate Sn-Se bond distance from the first peak distance of the total pair-correlation function $g(r)$ which is located at 2.68 Å. Bond distances Sn-Sn and Se-Se can indeed not be resolved experimentally as both contribute to a secondary broad peak at 3.88 Å. From the computed partial pair-correlation functions $g_{SnSn}(r)$ and $g_{SeSe}(r)$, one can see that the two distances are very close, i.e., $d_{Sn-Sn}=3.92$ Å against $d_{Se-Se}(r)=3.87$ Å (Table I). For the Sn-Se distance, the theory obtains 2.57 Å, somewhat lower than the experimental value of 2.68 found in the liquid.

In phase-change materials, one usually detects short and long distances between the nearest neighbors. This is found in, e.g., Ge-Sb-Te alloys for which a Peierls-type distortion mechanism[43] leads to different lengths for the Ge-Te bond. A similar situation prevails in SnSe$_2$. In fact, the detail of the local structures (Fig. 7) shows that the five-coordinated tin atoms (see the fraction of Sn^V below) have three bonds of approximately the same length (2.76 Å), one shorter (2.57 Å), and one longer bond (2.90 Å). The longer bond lies out of the equatorial plane and its bond angle with the latter is about 155°. Note that all these different bond lengths are all contained in the first peak of $g_{SnSe}(r)$. Similarly to other stoichiometric chalcogenides[18,39,44] (GeSe$_2$, GeS$_2$), the partials of Fig. 6 show prepeaks at short distances [e.g., $r=2.42$ Å in $g_{SeSe}(r)$] suggesting that a certain number of homopolar bonds exists in the liquid, mostly Se-Se bonds
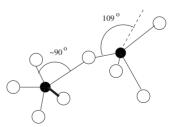

FIG. 7. Typical fivefold and fourfold tin atoms (in black) with their selenium neighbors, defining long and short (thick line) bonds and deviation from tetrahedral ordering (broken line, characterized by the 109° angle).
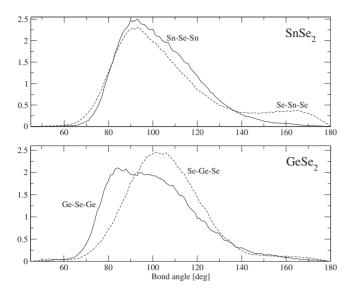
FIG. 8. Calculated bond angle distribution Sn-Se-Sn and Se-Sn-Se for SnSe$_2$ at 1173 K (upper panel). Calculated bond angle distribution Ge-Se-Ge and Se-Ge-Se for a corresponding liquid (Ref. 18) GeSe$_2$ system at 1050 K.

and to a lower extent Sn-Sn bonds. The latter produces only a shoulder on the principal peak, at around $r \simeq 3$ Å. Finally, we note the absence in the $g_{SnSn}(r)$ partial of a second typical shouldering in the principal peak of the $g_{SnSn}(r)$ partial. In experiments on GeSe$_2$, this feature is usually attributed[39] to shorter Ge-Ge distances that are found in edge-sharing GeSe$_{4/2}$ tetrahedra (ES or four rings). There are however a certain number of edge-sharing units (three four rings on average over the 40 ps trajectory) in the present simulated liquid as seen in Fig. 1. The nature of these rings is quite different from those obtained in *ab initio* studies of GeSe$_2$ which contribute in the Ge-Se-Ge bond angle distribution to a small peak at around 80° (Fig. 8). Indeed, the four rings in SnSe$_2$ form planar units having Sn-Se-Sn and Se-Sn-Se angles very close to 90° and whose contributions are merged with the ones arising from corner-sharing structures.

C. Coordination numbers and bond angle distributions

A simple inspection of the bond distances shows already that the liquid cannot be of tetrahedral nature as other group IV oxides or chalcogenides. Indeed, a perfect tetrahedron $AX_{4/2}$ has a distance ratio $\delta_A = d_{AX}/d_{XX}$ equal to $\sqrt{3/8} = 0.61$, a value that is found in experimental and/or simulated silica[45,46] ($\delta_{Si} = 0.62$) or germania[46,47] ($\delta_{Ge} = 0.62$), but also in other chalcogenides [e.g., $\delta_{Ge} = 0.63$ in GeSe$_2$ (Ref. 39)] where tetrahedral ordering prevails. For liquid SnSe$_2$, one obtains $\delta_{Sn} = 0.66$, a value that is comparable to densified silicas and germanias for which a tetrahedral to octahedral conversion under pressure occurs.[48,49] The corresponding densified structure of oxides at $\delta = 0.66$ contains already a certain fraction of higher-coordinated (5, 6) germanium[50] or silicon.[51] Thus SnSe$_2$ must contain higher-coordinated tin. From the partial coordination numbers n_{SnSn}, n_{SnSe}, and n_{SeSe} (Table I), the average coordination numbers n_{Sn} and n_{Se} for
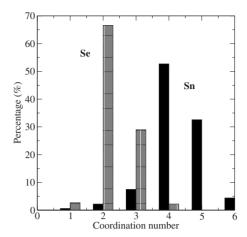

FIG. 9. Species of a given coordination number (percentage). A distance cutoff 3.1 Å has been used which corresponds to the first minimum in the Sn-Se pair-correlation function.

tin and selenium can be computed (Table I) and finally the mean coordination number $\bar{r}$ of the liquid,

$$n_{Sn} = n_{SnSn}^{(1)} + n_{SnSe} = 4.86,$$

$$n_{Se} = n_{SeSe}^{(1)} + n_{SeSn} = 2.49, \quad (3)$$

and

$$\bar{r} = c_{Sn}n_{Sn} + c_{Se}n_{Se} = 3.26, \quad (4)$$

while experimentally,[21] the nearest-neighbor coordination number is found to be $\bar{n} = 4.3$. A simple argument based on the 8-N rule would expect that for SnSe$_2$, $\bar{r} = 2.67$, a value that is very different from what has been obtained in Eq. (4). In fact, the 8-N rule breaks down because of the metallic character of tin that is even more increased in the liquid phase as manifested by an increase in electrical conductivity with temperature.[23]

Figure 8 shows the bond angle distributions (BADs) Se-Sn-Se and Sn-Se-Sn that provide additional information into the liquid topology. Here one can conclude that part of the atoms have a coordination number that is larger than four as the distributions peaks at 90°, similarly to what is expected when octahedra are present in the structure. This is also directly related to the corresponding crystalline phase for which the Se-Sn-Se bond angles are 90° (see below) and as Se atoms have six nearest neighbors, their coordination is perfectly octahedral. The Se-Sn-Se BAD displays two distinct contributions having a maximum at around 90° and a plateau somewhat lower than 180° (i.e., 165°). This suggests that the selenium atoms can either lie in an equatorial plane (90°) of a tin polyhedra or at its vertices (180°). Local distortion of the polyhedra brings to the departure from these "ideal" values such as shown in Fig. 7.

The present local structure does not display tetrahedral character which manifests by a BAD maximum at around 109°, a feature observed in silica, GeO$_2$ or in simulated GeSe$_2$ (Ref. 18) (dotted line in the bottom panel of Fig. 8). We finally compute the average number of Sn and Se atoms that are r-fold coordinated (Fig. 9). Here one sees that
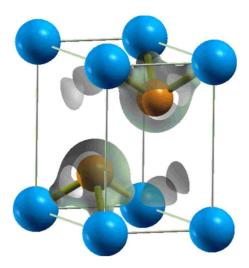
FIG. 10. (Color online) The hexagonal unit cell of the crystal-line phase. The transparent structure represents a charge-density isosurface. The eight Sn atoms are shown in blue and two Se atoms in orange.

the Sn atoms are mainly fourfold coordinated (52.7%) with a large fraction, however, of fivefold Sn that leads to the average value found in Eq. (3). One should note that in contrast with ordinary phase-changing materials (such as germanium tellurides) the fraction of octahedral sites is very low. As a consequence, it appears that the local tin structure is made of an octahedra with a vacancy found either in the equatorial plane or at the vertices. The selenium atoms display a majority of twofold atoms (68%) but with a large amount of threefolded defects that are reminiscent of the crystal phase. Other coordinations ($r=1$ or $r=4$) are lower than 5%.

IV. COMPARISON WITH THE CRYSTAL STRUCTURE

The structure of the crystal is displayed in Figs. 10 and 11. Figure 10 shows the hexagonal unit cell; Fig. 11 shows eight such cells revealing the layered structure of the crystal
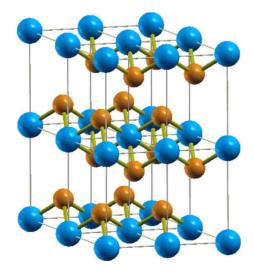

FIG. 11. (Color online) Snapshot of eight hexagonal unit cells (Sn atoms are shown in blue and Se in orange).

phase. The smallest structures are Sn_3Se pyramids, both corner-sharing as well as edge sharing. Only heteropolar bonds are present, with Se threefold coordinated and Sn six-fold coordinated. The bonding angles have been computed to 90.1° for Sn-Se-Sn and 89.9°, 90.1°, and 180° for Se-Sn-Se. The peak observed at 165° in the bond angle distribution of the liquid phase (Fig. 8) is not present in the crystal. The calculated atomic distances in GGA are given in Table I. The difference in the bond length between the experimental crystalline data and the GGA values amounts to 2.9% and is thus within the typical deviation margin found for *ab initio* calculations. As opposed to the experimental data, the calculations show a significant change in the Sn-Se bond length between the crystalline and the liquid phase. In the liquid the Sn-Se bonds contract by 0.19 Å from 2.76 to 2.57 Å. However, one should keep in mind that the evaluation of the experimental distance Sn-Se in the liquid has been obtained[21] from the total pair distribution function that was not able to separate the other distances involved [e.g., Sn-Sn(1) and Se-Se(1) of Table I]. Compared to the crystal the average coordination decreases in the liquid, where Sn becomes four-fold or fivefold coordinated, and a significant number of Se atoms switches from a threefold to a twofold coordination. This leads to local building blocks different from those found in the crystal. Furthermore the bond distortions found in the crystalline phase of many phase-change alloys such as the GeSbTe compounds[12] are not found in $SnSe_2$. Hence on average the coordination number in the crystal is 4 and thus higher than for typical crystalline phase-change materials, where it is normally in the range of three (see, e.g., Ref. 52). As in the liquid it does not follow the 8-N rule. The bonding has been explained as being governed by an incomplete sp^3 hybridization for Se and by resonating sp^3d^2 bonds for Sn.[53] After displacing the atoms they move back to the original lattice sites during the structural relaxation.

The volume contraction calculated from the experimental data from Refs. 21 and 42 amounts to 18%, thus comparable to the 17% reported for the volume contraction between the amorphous and the crystalline state.[10] In the calculations, the density of the liquid has to be fixed to the experimental value, while the crystal structure relaxes significantly resulting in a mere volume contraction between liquid and crystalline phase of 8.5%. Nevertheless, the calculations elucidate some of the origins of the volume contraction. The coordination number decreases in the liquid while the bond angles increase on average. The lower coordination number consequently results in a lower density in the liquid while the remaining heteropolar bonds become stronger and therefore shorter. Experimental data[23] on liquid $SnSe_2$ show that some thermodynamic quantities evolve very rapidly when the temperature is increased. In fact, the excess mixing volume displays a very large difference with temperature whereas it is almost the same for selenium-rich and tin-rich liquids. Temperature-composition studies in Sn_xSe_{1-x} liquids show furthermore large adiabatic compressibility and thermal-expansion coefficient change at $x=0.33$. These data indicate that the liquid phase exhibits unique structural properties different from the crystal and amorphous phase.

V. SUMMARY AND CONCLUSIONS

In this paper, we have presented an *ab initio* molecular dynamics study of liquid and crystalline $SnSe_2$. It is the study of this system from molecular simulations and represents an interesting means to analyze in a more deeper fashion the experimental data obtained from neutron diffraction. We have shown that in liquid $SnSe_2$, a majority of twofolded selenium atoms could be found with a minority of atoms in threefold coordination. The latter corresponds to the coordination of the crystal. Tin atoms display an even more profound change as Sn is octahedral in c-$SnSe_2$ and four- and five-coordinated in the liquid. However, the structure is not tetrahedral as bond angle distribution does not display a maximum at the usual angle of 109° for the Se-Sn-Se bonds. Instead, a maximum at 90° is found, together with a plateau at around 160°. These values correspond either to a (angle and bond) distorted tetrahedron or to a five-coordinated tin atom having four selenium atoms in an approximate equatorial plane with a fifth selenium atom lying at the vertex of the polyhedra.

Finally, we stress that the structure of liquid $SnSe_2$ should be rather different from the crystalline and amorphous counterparts. Indeed, due to the large volume differences between these three states of matter and the effect of cell volume change in simulation on the short and intermediate range orders, we do expect that the coordination distribution such as the one displayed in Fig. 9 should depend substantially on temperature. This issue is presently under consideration.

[1] M. Wuttig and N. Yamada, Nature Mater. **6**, 824 (2007).

[2] M. Libera and M. Chen, J. Appl. Phys. **73**, 2272 (1993).

[3] N. Yamada, MRS Bull. **21**, 48 (1996).

[4] S. R. Ovshinsky, Phys. Rev. Lett. **21**, 1450 (1968).

[5] S. Hudgens and B. Johnson, MRS Bull. **29**, 829 (2004).

[6] A. Greer and N. Mathur, Nature (London) **437**, 1246 (2005).

[7] T. Grosges, S. Petit, D. Barchiesi, and S. Hudlet, Opt. Express **12**, 5987 (2004).

[8] M. H. R. Lankhorst, B. W. S. M. M. Ketelaars, and R. A. M. Wolters, Nature Mater. **4**, 347 (2005).

[9] D. Milliron, S. Raoux, R. Shelby, and J. Jordan-Sweet, Nature Mater. **6**, 352 (2007).

[10] Kyung-Min Chung, D. Wamwangi, M. Woda, M. Wuttig, and W. Bensch, J. Appl. Phys. **103**, 083523 (2008).

[11] M. H. R. Lankhorst, J. Non-Cryst. Solids **297**, 210 (2002).

[12] M. Wuttig, D. Lüsebrink, D. Wamwangi, W. Welnic, M. Gillessen, and R. Dronskowski, Nature Mater. **6**, 122 (2007).

[13] *Insulating and Semiconducting Glasses*, edited by P. Boolchand (World Scientific, Singapore, 2000).

[14] W. Njoroge, H. W. Wöltgens, and M. Wuttig, J. Vac. Sci. Technol. A **20**, 230 (2002).

[15] J. Kalb, M. Wuttig, and F. Spaepen, J. Mater. Res. **22**, 748 (2007).

[16] P. Vashishta, R. K. Kalia, G. A. Antonio, and I. Ebbsjö, Phys. Rev. Lett. **62**, 1651 (1989); P. Vashishta, R. K. Kalia, and I. Ebbsjö, Phys. Rev. B **39**, 6034 (1989); H. Iyetomi, P. Vashishta, and R. K. Kalia, *ibid.* **43**, 1726 (1991).

[17] J. C. Mauro and A. K. Varshneya, J. Am. Ceram. Soc. **89**, 2323 (2006).

[18] C. Massobrio, A. Pasquarello, and R. Car, Phys. Rev. B **64**, 144205 (2001).

[19] C. Massobrio, A. Pasquarello, and R. Car, J. Am. Chem. Soc. **121**, 2943 (1999).

[20] M. Cobb and D. A. Drabold, Phys. Rev. B **56**, 3054 (1997).

[21] K. Itoh, K. Maruyama, M. Misawa, and S. Tamaki, J. Phys. Soc. Jpn. **69**, 1717 (2000).

[22] M. Popescu, F. Sava, A. Lörinczi, G. Socol, I. N. Mihailescu, A. Tomescu, and C. Simion, J. Non-Cryst. Solids **353**, 1865 (2007).

[23] F. Kakinuma, Y. Tsuchiya, and K. Suzuki, J. Phys. Soc. Jpn. **66**, 3859 (1997).

[24] R. Car and M. Parrinello, Phys. Rev. Lett. **55**, 2471 (1985).

[25] J. P. Perdew and A. Zunger, Phys. Rev. B **23**, 5048 (1981).

[26] A. D. Becke, Phys. Rev. A **38**, 3098 (1988); C. Lee, W. Yang, and R. G. Parr, Phys. Rev. B **37**, 785 (1988).

[27] F. H. M. van Roon, C. Massobrio, E. de Wolff, and S. W. de Leeuw, J. Chem. Phys. **113**, 5425 (2000).

[28] C. Massobrio, F. H. M. van Roon, A. Pasquarello, and S. W. de Leeuw, J. Phys.: Condens. Matter **12**, L697 (2000).

[29] G. Ferlat and M. Micoulaut, Glass Sci. Technol. (Amsterdam, Neth.) (to be published).

[30] X. Gonze *et al.*, Comput. Mater. Sci. **25**, 478 (2002).

[31] The ABINIT code is a common project of the Universite Catholique de Louvain, Corning, Incorporated, the Universite de Liege, the Commissariat a l'Energie Atomique, Mitsubishi Chemical Corp., the Ecole Polytechnique Palaiseau, and other contributors (http://www.abinit.org).

[32] J. P. Perdew, K. Burke, and M. Ernzerhof, Phys. Rev. Lett. **77**, 3865 (1996).

[33] C. Bichara, M. Johnson, and J. P. Gaspard, Phys. Rev. B **75**, 060201(R) (2007).

[34] C. Steimer, M.-V. Coulet, W. Welnic, H. Dieker, R. Detemple, C. Bichara, B. Beuneu, J. P. Gaspard, and M. Wuttig (unpublished).

[35] A. B. Bhatia and D. E. Thornton, Phys. Rev. B **2**, 3004 (1970).

[36] P. S. Salmon, R. A. Martin, P. E. Mason, and G. J. Cuello, Nature (London) **435**, 75 (2005).

[37] P. S. Salmon, J. Phys.: Condens. Matter **18**, 11443 (2006).

[38] P. S. Salmon, A. C. Barnes, R. A. Martin, and G. J. Cuello, Phys. Rev. Lett. **96**, 235502 (2006).

[39] P. S. Salmon, Proc. R. Soc. London, Ser. A **437**, 591 (1992).

[40] C. Massobrio and A. Pasquarello, Phys. Rev. B **77**, 144207 (2008).

[41] S. Susman, K. J. Volin, D. G. Montague, and D. L. Price, Phys. Rev. B **43**, 11076 (1991).

[42] W. B. Pearson, *The Crystal Chemistry and Physics of Metals and Alloys* (Wiley, New York, 1972).

[43] J. Y. Raty, V. Godlevsky, P. Ghosez, C. Bichara, J. P. Gaspard, and J. R. Chelikowsky, Phys. Rev. Lett. **85**, 1950 (2000).

[44] I. Petri and P. S. Salmon, J. Non-Cryst. Solids **293-295**, 169 (2001).

[45] D. I. Grimley, A. C. Wright, and R. N. Sinclair, J. Non-Cryst. Solids **119**, 49 (1990).

[46] M. Micoulaut, J. Phys.: Condens. Matter **16**, L131 (2004).

[47] D. L. Price, M. L. Saboungi, and A. C. Barnes, Phys. Rev. Lett. **81**, 3207 (1998).

[48] J. P. Itie, A. Polian, G. Calas, J. Petiau, A. Fontaine, and H. Tolentino, Phys. Rev. Lett. **63**, 398 (1989).

[49] K. Trachenko and M. T. Dove, J. Phys.: Condens. Matter **14**, 1143 (2002).

[50] M. Micoulaut, X. Yuan, and L. W. Hobbs, J. Non-Cryst. Solids **353**, 1961 (2007).

[51] V. V. Brazhkin and A. G. Lyapin, J. Phys.: Condens. Matter **15**, 6059 (2003).

[52] W. Wełnic, A. Pamungkas, R. Detemple, C. Steimer, S. Blügel, and M. Wuttig, Nature Mater. **5**, 56 (2006).

[53] M. Schlüter and Marvin L. Cohen, Phys. Rev. B **14**, 424 (1976).